

Does Better Tropospheric Circulation Bring Better QBO?

Project Representative

Shingo Watanabe Research Center for Environmental Modeling and Application,
Research Institute for Global Change, Japan Agency for Marine-Earth Science and
Technology

Authors

Shingo Watanabe *¹, Yoshio Kawatani *^{2,1}

*¹ Research Center for Environmental Modeling and Application, Research Institute for Global Change, Japan Agency for Marine-Earth Science and Technology, *²Faculty of Environmental Earth Science, Hokkaido University

Keywords : Middle atmosphere, Climate modeling, Quasi-biennial oscillation

1. Introduction

More than 60 years have passed since the quasi-biennial oscillation (QBO) was first discovered in the equatorial lower stratosphere [1][2]. Additionally, it has been almost three decades since it was first simulated in atmospheric general circulation models (AGCMs) [3]. During this period, significant progress has been made in our understanding of the mechanisms that drive the QBO and the recipes and cookbooks for reproducing it with AGCMs [4]

Traditionally, modelers have tried to improve the stratospheric processes of AGCMs to have better representation of the QBO. This improvement involves increasing vertical resolution of the stratosphere and incorporating non-orographic gravity wave parameterizations. On the other hand, there has been limited research on how the adequacy of the tropospheric circulations in models influences the reproducibility of the QBO. In this study, we will demonstrate how nudging the troposphere of AGCMs changes the simulated QBO. We are, of course, interested in the mechanisms that bring about such changes.

2. Method

The results are model-dependent, so a multi-model approach is preferred. As a starting point, two AGCMs were prepared as the minimum set for this study. Here, the models A and B are similar but use different cumulus convection schemes.

2.1 Models

- Model-A – used in SPARC-QBOi2

MIROC6.1-AGCM with a T85 (~1.4deg) horizontal resolution is the developer's version of MIROC-AGCM, which bridges CMIP6 and CMIP7, with some minor updates from MIROC6.0 [5].

- Model-B

The Chikira-Sugiyama (2010) cumulus scheme [6] used in Model A is switched to the mass-flux prognosed-type Arakawa-Schubert scheme [7][8].

Both models have differently tuned to obtain as realistic QBO period and amplitude as possible. - The most important parameter

was the constant source for the non-orographic gravity wave parameterization of Hines (1997) [9].

2.2 Experiments

- Control experiments

Using both models, 28 years of AMIP experiments (Exp1 in QBOi [10]) were conducted from the beginning of 1979 to the end of 2006, which may contain ~12 QBO cycles as observed. These experiments started from the same initial conditions at the beginning of 1979, in which the QBO zonal winds were initialized using ERA5 [11]. The external forcing including the sea surface temperature, sea-ice concentration, and greenhouse gas concentrations, etc. followed the historical forcing provided by CMIP6.

- Tropospheric spectral nudging (TSN) experiments

We wanted to correct biases in the large-scale circulation, including broad structures of the Walker circulation, in the troposphere and let the atmospheric waves behave as freely as possible. To do this, we conducted spectral nudging experiments, applying nudging throughout the atmosphere below 100 hPa in both models utilizing the total horizontal wavenumber 0-10 components of the 3-dimensional daily horizontal winds from ERA5, with a relaxation time constant of 1 day.

3. Results

3.1 Biases in the Upper Tropospheric Walker Circulation

Fig. 1 compares the seasonal march of the upper branch of the Walker circulation in both models with ERA5. The strong and wide easterly wind bias in the eastern hemisphere (EH) is most

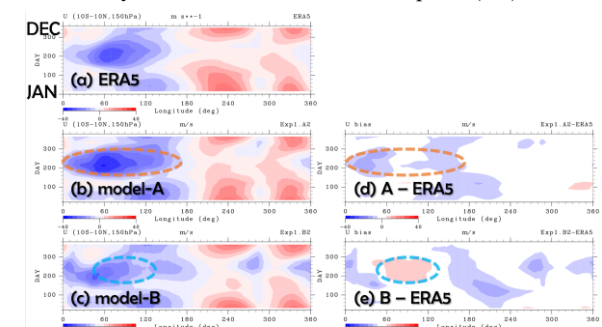


Fig.1: Hovmöller diagram of equatorial (10S-10N) averaged monthly mean 150 hPa eastward winds, averaged for 1979-2006. (a) ERA5, (b) model-A, (c) model-B, (d) A - ERA5, (e) B - ERA5.

prominent in July of Model A. In contrast, easterly wind speed in July of Model B is underestimated over the Indian Ocean. These wind biases are greatly improved with TSN (not shown).

3.2 Changes by Tropospheric Spectral Nudging

Fig. 2 compares the time evolution of the zonal mean zonal wind profiles in the equatorial lower stratosphere for both models with ERA5. The mean period of QBO is well reproduced in the models. The QBO period in Model-A increased with TSN (~28 => ~31 mo). In contrast, it decreased in Model-B (~26 => ~24 mo). Are these changes related to the Walker circulation biases which peaks in July?

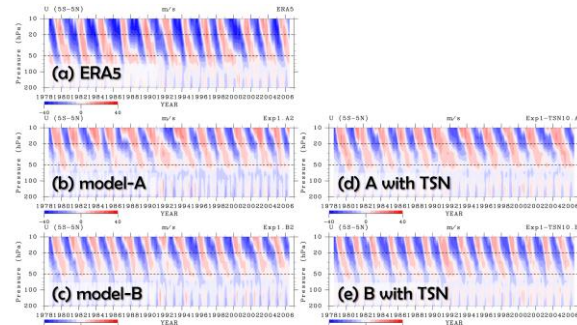


Fig.2: Time-height diagram of equatorial (5S-5N) averaged monthly mean zonal mean eastward winds for 1979-2020. (a) ERA5, (b) model-A, (c) model-B, (d) A with TSN, (e) B with TSN.

3.3. Zonal Wind Forcing by Resolved Waves

Figs. 3a-b compare the longitude-height distribution of eastward forcing due to resolved waves in July 1979, calculated according to the divergence of the 3D wave activity fluxes of Miyahara (2006) using the 1-hour interval output of each model. The eastward (positive) wave forcing in Model A in the EH middle stratosphere (10-30hPa; blue box) is stronger than that in Model B. The contours of zonal winds strangely bend down in the blue box in Fig. 3a.

Figs. 3c-d shows results in the TSN experiment where the tropospheric circulation biases were corrected by the spectral nudging. The eastward wave forcing in the EH middle stratosphere (10~30 hPa: blue boxes) decreases in Model A as the easterly winds in the upper troposphere weaken by TSN. On the contrary, it increases in Model B as the easterly winds in the upper troposphere strengthens by TSN. For the westward wave

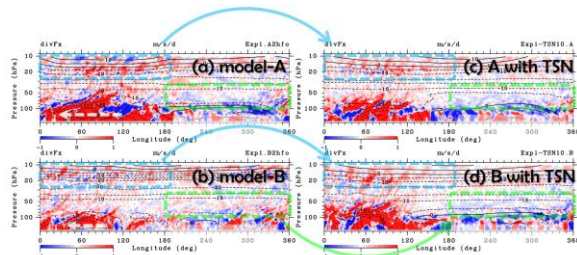


Fig.3: Longitude-height diagram of equatorial (10S-10N) averaged monthly mean eastward winds (contours) and $\nabla \cdot F_x$ (shadings; positive = eastward) in July 1979. (a) model-A, (b) model-B, (c) A with TSN, (d) B with TSN.

forcing in the WH lower stratosphere (40-100 hPa: green boxes), it increases in Model B as the westerly winds in the upper troposphere strengthens.

3.4. k - ω Spectrum of u' & w' at 70 hPa

Fig. 4 shows the zonal wavenumber (k)-frequency (ω) cross spectra for the eastward wind (u) and vertical wind (w) fluctuations, corresponding to the vertical flux of zonal momentum due to atmospheric waves. In the k - ω space, red shadings show the eastward momentum flux due to eastward propagating waves relative to weak easterlies, which cause the eastward wave forcing in the EH middle stratosphere (blue boxes in Fig. 3). Blue shadings show the westward momentum flux due to westward propagating waves relative to the weak easterlies, which cause the westward wave forcing in the WH lower stratosphere (green boxes in Fig. 3).

With TSN, the eastward momentum flux decreases in $-10 < C_x < 20 \text{ ms}^{-1}$ in Model A, where C_x denotes the zonal phase speed relative to the ground. When we examine the k - ω spectra for precipitation, its power spectral density rather increases in that phase speed range (not shown). Presumably, it would be attributable to a reduction in obstacle effect generation of GWs associated with the reduction of easterly wind speed in the EH upper troposphere. In contrast, the magnitude of zonal momentum flux increases in $-20 < C_x < 5 \text{ ms}^{-1}$ in Model B, which may be attributable to the strengthening of the upper tropospheric

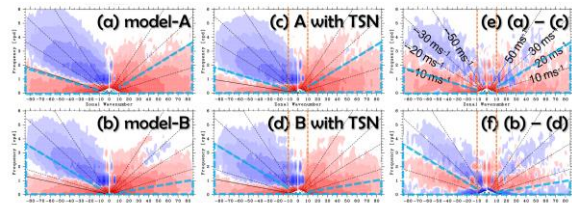


Fig.4: Zonal wavenumber (k) - frequency (ω) cross spectrum of u and w at 70 hPa in July 1979. The range of shadings is $-1e^4 - 1e^4 \text{ [Pa } k^{-1} \text{ cpd}^{-1}]$. Warm (cold) colors denote vertical flux of eastward (westward) momentum. (a) model-A, (b) model-B, (c) A with TN, (d) B with TN, (e) (a) - (c), and (f) (b) - (d).

easterly winds over the Indian Ocean.

4. Summary and Discussions

By conducting the tropospheric spectral nudging experiments, this study demonstrated that the bias of the upper branch of the Walker circulation in the EH had a significant impact on the QBO period simulated by the model through the changes in the resolved wave forcing:

Weaker Walker circulation -> weaker GW generation -> less GW forcing on QBO-> longer QBO period.

In this study, we only present the results of the wave analysis focused on July of the first year of the 28 years of continuous integration. This is because July was the month in which the model's Walker circulation bias was largest, and because we wanted to have a similar QBO phase in each run for the comparison.

To gain more useful insight into how to improve the QBO in

AGCMs with seasonal biases in tropospheric (and stratospheric) circulation, we propose, for example, to compare the momentum budget of the QBO zonal wind with reanalysis products by conducting a series of one-month hindcast experiments starting from the beginning of every month during the typical QBO cycle, e.g., 1981-1983. The TSN and 3D wave analysis may be worth to combine with such a Transpose-AMIP type approach with more intention on shorter time scale than we have done in the multi-model seasonal hindcasts of the QBO: SPARC QBOi-Exp5 (Stockdale et al., 2020). We have conducted such experiments using MIROC6.1 and the GW-permitting Japanese AGCM for Upper Atmosphere Research (JAGUAR) and results would be reported in the near future.

Acknowledgement

This study was supported by JSPS-KAKENHI (JP22H01303) & MEXT-Program for the advanced studies of climate change projection (SENTAN) (JPMXD0722681344). Numerical simulations were conducted using the Earth Simulator at JAMSTEC. The DCL-DENNOU Library and GTOOL were used for analysis and visualization.

References

- [1] Baldwin, M. P., et al. (2001), The quasi-biennial oscillation, *Rev. Geophys.*, 39(2), 179–229, doi:10.1029/1999RG000073.
- [2] Anstey, J.A., Osprey, S.M., Alexander, J. et al. (2022) “Impacts, processes and projections of the quasi-biennial oscillation,” *Nat Rev Earth Environ* 3, 588–603. <https://doi.org/10.1038/s43017-022-00323-7>
- [3] Takahashi, M. (1996), Simulation of the stratospheric Quasi-Biennial Oscillation using a general circulation model, *Geophys. Res. Lett.*, 23(6), 661-664, <https://doi.org/10.1029/95GL03413>
- [4] Garfinkel, C. I., Gerber, E. P., Shamir, O., Rao, J., Jucker, M., White, I., & Paldor, N. (2022). A QBO cookbook: Sensitivity of the quasi-biennial oscillation to resolution, resolved waves, and parameterized gravity waves. *Journal of Advances in Modeling Earth Systems*, 14, e2021MS002568. <https://doi.org/10.1029/2021MS002568>
- [5] Tatebe, H., Ogura, T., Nitta, T., Komuro, Y., Ogochi, K., Takemura, T., Sudo, K., Sekiguchi, M., Abe, M., Saito, F., Chikira, M., Watanabe, S., Mori, M., Hirota, N., Kawatani, Y., Mochizuki, T., Yoshimura, K., Takata, K., O'ishi, R., Yamazaki, D., Suzuki, T., Kurogi, M., Kataoka, T., Watanabe, M., and Kimoto, M. (2019), Description and basic evaluation of simulated mean state, internal variability, and climate sensitivity in MIROC6, *Geosci. Model Dev.*, 12, 2727–2765, <https://doi.org/10.5194/gmd-12-2727-2019>
- [6] Chikira, M., and M. Sugiyama (2010), A Cumulus Parameterization with State-Dependent Entrainment Rate. Part I: Description and Sensitivity to Temperature and Humidity Profiles. *J. Atmos. Sci.*, 67, 2171–2193, <https://doi.org/10.1175/2010JAS3316.1>.
- [7] Arakawa, A., and W. H. Schubert, 1974: Interaction of a Cumulus Cloud Ensemble with the Large-Scale Environment, Part I. *J. Atmos. Sci.*, 31, 674–701, [https://doi.org/10.1175/1520-0469\(1974\)031<0674:IOACCE>2.0.CO;2](https://doi.org/10.1175/1520-0469(1974)031<0674:IOACCE>2.0.CO;2)
- [8] Emori, S., Nozawa, T., Numaguchi, A., and Uno, I. (2001), Importance of cumulus parameterization for precipitation simulation over East Asia in June, *J. Meteorol. Soc. Jpn*, 79(4), 939-947, <https://doi.org/10.2151/jmsj.79.939>
- [9] Hines, C. O. (1997), Doppler-spread parameterization of gravity-wave momentum deposition in the middle atmosphere. Part 2: Broad and quasi monochromatic spectra, and implementation, *J. Atmos. Sol-Terr. Phys*, 59 (4), 378-400, [https://doi.org/10.1016/S1364-6826\(96\)00080-6](https://doi.org/10.1016/S1364-6826(96)00080-6)
- [10] Butchart, N., Anstey, J., Hamilton, K. Osprey, S., McLandress, C., Bushell, A., Kawatani, Y., Kim Y-H, Lott, F., Scinocca, J., Stockdale, T., Bellprat, O., Braesicke, P., Cangirosso, B., Chen, C-C., Chun, H-Y., Dobrynin, M., Garcia, R., Garcia-Serrano, J., Gray, L., Holt, L., Kerzenmacher, T., Naoe, H., Pohlmann, H., Ritcher, J., Scaife, A., Schenzinger, V., Serva, F., Versick S., Watanabe, S. Yoshida, K. and Yukimoto, S., (2018), Overview of experiment design and comparison of models participating in the SPARC Quasi-Biennial Oscillation initiative (QBOi), *Geosci. Model. Dev.*, 11, 1009-1032, <https://doi.org/10.5194/gmd-11-1009-2018>
- [11] Hersbach, H., et al. (2020), The ERA5 global reanalysis, *Q. J. Roy. Met. Soc.*, 146(730), 1999-2049, <https://doi.org/10.1002/qj.3803>